Diffusional Creep: Stresses and Strain Rates in Thin Films and Multilayers

D. Josell, T.P. Weihs, and H. Gao

Abstract

In this article, we discuss creep deformation as it relates to thin films and multilayer foils. We begin by reviewing experimental techniques for studying creep deformation in thin-film geometries, listing the pros and cons of each; then we discuss the use of deformation-mechanism maps for recording and understanding observed creep behavior. We include a number of cautionary remarks regarding the impact of microstructural stability, zero-creep stresses, and transient-creep strains on stress–strain rate relationships, and we finish by reviewing the current state of knowledge for creep deformation in thin films. This includes both thin films that are heated on substrates as well as multilayer films that are tested as freestanding foils.

Keywords: *diffusional creep, mechanical properties, thin films.*

Introduction

In studying the mechanical properties of materials, most researchers emphasize yield or fracture properties and test for these quantities using simple tension tests and bend tests. However, while yield strength and fracture toughness are useful properties for designing materials and structures, they are rarely experienced in applications involving thin films and multilayers.

On the other hand, many materials do exhibit time-dependent deformation, or creep, under stresses well below those needed to cause yielding or fracture. This time-dependent deformation occurs by means of a variety of deformation processes. In thin-film applications, creep deformation is often driven by stresses that arise from mismatched thermal expansions of a film and the substrate on which it is deposited. Stress relaxation by means of creep deformation is ubiquitous in the processing of multilevel, thin-film devices that require multiple processing steps at numerous temperatures. Because rates for several creep mechanisms increase rapidly as grains get smaller, they cannot be ignored in thin-film structures, even at room temperature. We therefore discuss creep deformation as it relates to homogeneous films on substrates and stacked thin films, or so-called multilayers.

As noted in other articles in this issue, atomistic simulations have become an important resource for modeling a large number of deformation processes. However, even with recent increases in computational speed, simulations are limited to extreme cases of total strain or strain rate that do not yet yield useful predictions in the case of creep deformation. To predict plastic strains of a realistic magnitude, one is restricted to strain rates of $10^7\ \mathrm{s}^{-1}$ or higher[1] that are many orders of magnitude greater than experimental strain rates. Alternatively, if realistic strain rates are used (10^{-5}–$10^{-9}\ \mathrm{s}^{-1}$), creep strains are limited to magnitudes ($\leq 10^{-12}$) that are far too small to be informative. Therefore, this article focuses on experimental techniques and analytical models for characterizing creep deformation in thin films.

In keeping with the goal of this issue of *MRS Bulletin,* we emphasize areas where unique issues arise due to the thin-film geometries being addressed. We first note some of the techniques used to study creep in thin films. We then discuss stress development during film growth, microstructural stability during creep tests, and the relationships between applied stresses, strain rates, microstructures, and deformation mechanisms. We next outline zero-creep stresses and transient strains that must be considered when evaluating creep properties, noting their impact on thin-film creep tests. Finally, we discuss creep deformation of films on substrates and freestanding multilayer films.

Test Techniques

As with bulk specimens, simple tension tests are one technique for studying creep properties. Films can be released from their substrates and tested in tension as completely freestanding samples[2,3] or in bending as cantilever structures.[4] Such tests involve challenging sample preparation and handling. However, they permit accurate, independent control of applied stress and test temperature during creep studies.

More commonly, creep deformation in thin films is studied while they remain on a substrate that deforms only elastically.[5] These studies utilize film stresses that arise due to mismatched thermal expansions or contractions of the substrate and film. Since these samples require little preparation other than deposition, this geometry is convenient. However, it does not permit independent control of temperature, stress, or strain. As a result, creep studies at fixed stresses are not possible.

A hybrid test method that falls midway between these two techniques involves tensile tests of films on substrates that can deform plastically. This method reduces the coupling of film stress, strain, and temperature while easing the handling of samples.[6] However, temperatures in such tests are limited by the polymeric nature of the substrates. In nanoindentation creep tests, one can control loading.[7–10] The complex nature of the stress state under the indenter tip requires significant modeling, however, which introduces significant uncertainties into the values of materials properties thus obtained.

Regardless of the experimental technique used, the goal of thin-film creep studies is to experimentally measure creep rates and identify creep mechanisms for a range of applied stresses and temperatures using specimens that are well defined chemically and microstructurally.

Creep of Thin Films

Creep during Film Growth

Creep deformation often first appears during the growth of thin films due to the development of large stresses during deposition. The significant role of diffusional processes in the relaxation of these stresses is discussed in the article in this issue by Floro et al.

Stability of the Thin-Film Structure

Since most thin films are deposited with fine microstructures and metastable phases, both chemical and microstructural stabilities are major concerns when characterizing creep rates and mechanisms. Creep conditions are usually chosen to avoid conditions where phase transformations or substantial microstructural evolution (e.g., the breakdown of a multilayer into discontinuous layers) occur very rapidly. Otherwise, interpretation of creep properties is complicated by the need to correlate the measured properties with the changing microstructure of the system.

Assuming the phases in thin films and multilayers are chemically stable, diffusional processes play a significant role in determining the stability of their microstructures because they control the kinetics of grain growth, grain-boundary grooving (see Figure 1), and pit formation at triple junctions. The energetics and kinetics of microstructural stability in polycrystalline thin films on substrates can be found in several works,[11–15] as can studies of stability in multilayer specimens.[16–20] Generally, a thin film is predicted to be more stable energetically if it has grain boundaries with free energies that are low compared with the free energy of the film surface. Similarly, a multilayer is predicted to be more stable energetically if it has grain boundaries with free energies that are low compared with the free energy of the interfaces between layers. Energetic stability should be enhanced if in-plane grain sizes are not significantly larger than the film or layer thickness; stability should thus benefit from stagnation of in-plane coarsening. Kinetically, instabilities such as deep pits or grooves will form more slowly when diffusional transport is slow.

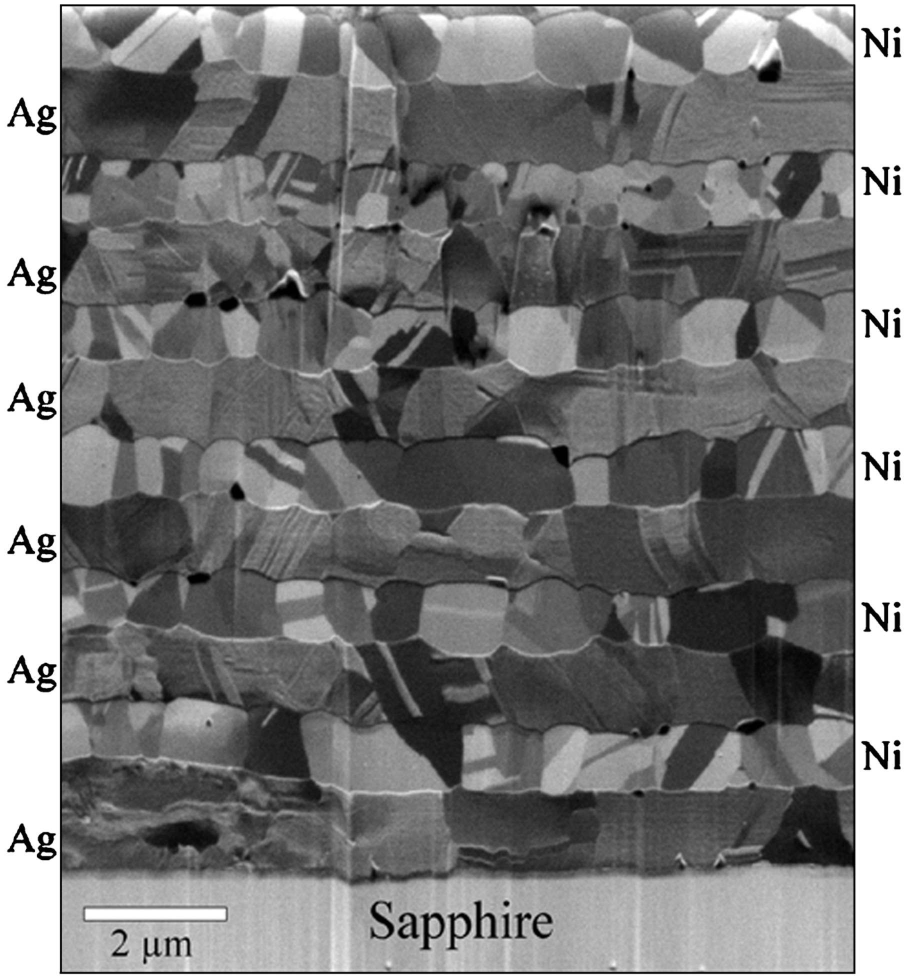

Figure 1. Cross section of a Ag/Ni multilayer on a thin sapphire substrate after 24 h of biaxial zero-creep testing at 500°C.[20] The image was obtained using secondary electron imaging after focused-ion-beam milling. Note the significant grooving into the Ni layers where the Ni grain boundaries meet the Ag/Ni interfaces. (Imaging and milling courtesy of A. Wilson and G. Spanos, Naval Research Laboratory, who gratefully acknowledge support from the Office of Naval Research.)

Creep-Deformation Mechanisms

Creep behavior in bulk or thin-film materials can be summarized by an empirical equation of the form[21]

$$\dot{\varepsilon} \equiv \frac{d\varepsilon}{dt} = A\frac{D}{\Omega^{2/3}}\left(\frac{\sigma}{G}\right)^{m}\left(\frac{\sigma\Omega}{kT}\right)\left(\frac{b}{d}\right)^{n}, \qquad (1)$$

describing the dependence of the creep rate $\dot{\varepsilon}$ of a material subject to a fixed applied stress σ. The power of that dependence is $m + 1$; A is a coefficient that depends on temperature and microstructure; D is a coefficient for diffusion through the bulk of a grain, along grain boundaries, or along dislocation cores; Ω is atomic volume, G is the shear modulus; k is the Boltzmann constant; T is temperature; b is the Burgers vector; and d is grain size. Different mechanisms control the creep deformation of a given material at different stresses and temperatures. Most broadly, at high stresses dislocation motion controls deformation, and power-law (dislocation) creep dominates; at low stresses atomic diffusion controls deformation, and diffusional creep dominates. Dislocation creep is controlled by dislocation glide at low homologous temperatures and by dislocation climb at high homologous temperatures. Similarly, diffusional-creep processes are controlled by diffusion along grain boundaries (Coble creep) at low homologous temperatures and by diffusion through the bulk of grains (Nabarro–Herring creep) at high temperatures. Typical values for A, m, and n are given in Table I for the different mechanisms. Note that the diffusional-creep mechanisms exhibit a strong grain-size dependence, indicated by the nonzero value of n, while the power-law-creep mechanisms do not. Diffusional creep is thus expected to dominate deformation in thin films with sufficiently small grain sizes. Considering in-plane grain size and film thickness as separate length scales[22] usually does not change this because in-plane grain size typically scales with film thickness.

In an effort to help identify the dominant creep mechanisms over the full range of achievable stresses and temperatures, Frost and Ashby developed the concept of

Table I: Parameters for the Generalized Creep Equation.

Mechanism	Conditions	A*	m*	n*
Nabarro–Herring creep	High temperature, low stress	7	0	2
Coble creep	Moderate temperatures, low stress, fine grain sizes	50	0	3
Power-law creep	Low to moderate temperatures, high stress	**	2–6	0

* *A* is a coefficient that depends on temperature and microstructure, while *m* and *n* are empirically derived constants.
** The values of *A* vary dramatically, depending on the microstructure that is controlling the power-law creep.

deformation-mechanism maps.[23] A deformation map for Ni is shown in Figure 2. These maps are based on diffusion data as well as experimental data from creep studies. Different maps are required for materials with different grain sizes. This particular map predicts the controlling creep mechanisms for Ni with a 1.0-μm grain size. The data used to predict many of these maps, particularly for the diffusional-deformation mechanisms, are frequently limited in quantity. As an example, Frost and Ashby based the Coble creep fields of their deformation maps for the fcc metals upon diffusion data rather than experimental creep data. The corresponding Nabarro–Herring creep fields are based on limited creep data at high temperatures. Predictions of such deformation maps for Coble and Nabarro–Herring creep-deformation fields should thus be considered qualitative rather than quantitative, particularly for materials with grain sizes significantly smaller than those available when the maps were developed. As Frost and Ashby noted, "The maps are no better (and no worse) than the equations and data used to construct them."[23]

Zero-Creep Stress

A creep property that is unique to small structures such as thin films and multilayers is the existence of a significant range of stresses for which a positive stress results in a negative strain rate. This occurrence, described empirically by an expression of the type

$$\dot{\varepsilon} \sim (\sigma - \sigma_0), \qquad (2)$$

is a manifestation of the drive to reduce the area, and thus the free energy, of the surfaces of a thin film[11] or the interfaces in a multilayer.[24–26] Figure 3 (from Reference 25) shows experimental creep data from Ag/Ni multilayers at different applied stresses (Figure 3a) from which strain rate versus stress-dependence (Figure 3b), and thus the zero-creep stress σ_0, can be determined. The value of σ_0 can also be derived through equilibrium thermodynamics arguments. An approximate value can be obtained from $\sigma_0 \approx \gamma/t$, where γ is the free energy of the surface (thin film) or interface (multilayer) and t is the thickness of the film or layer. Using $\gamma \approx 1$ J/m, σ_0 is only 1 MPa for $t = 1$ μm, but it is 100 MPa for $t = 10$ nm. *In situ* transmission electron microscope studies of creep of gold thin films found that inclusion of a zero-creep stress σ_0 of the order of 100 MPa explained why creep rates were ≈10,000× smaller than those predicted for the specimen geometry and test conditions.[27] Similarly, substrates on which multilayer films are deposited have been shown to relax to a nonzero equilibrium curvature due to the interfaces in the multilayer film.[28] Accounting for zero-creep stresses can be necessary for accurate interpretation of creep data of thin films and multilayers.

Steady-State versus Transient Creep

Creep rates depend on the magnitude of the cumulative creep and thus are not always constant for a given applied load or stress. This effect is well known for bulk structural materials at high temperatures ($T \geq 0.5T_m$), where creep has been studied for many decades. As is shown in Figure 4 for an FeCo intermetallic alloy thin film,[29] creep data are usually separated into three

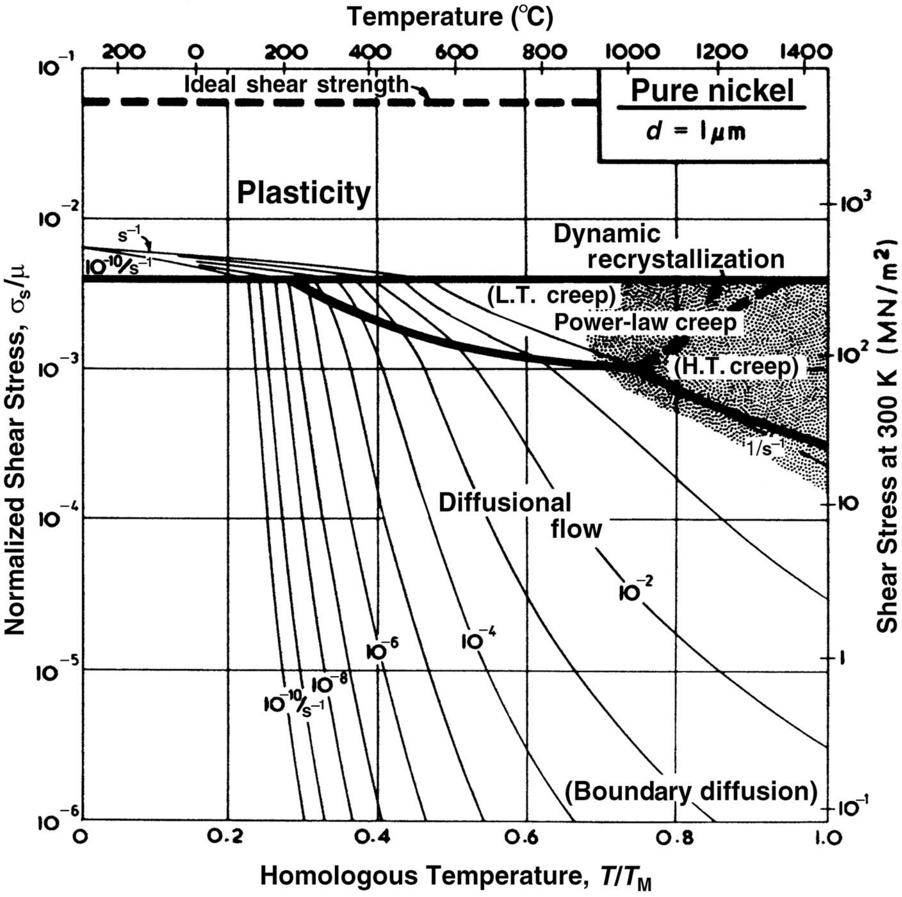

Figure 2. A deformation-mechanism map for Ni composed of 1.0-μm grains (from Reference 23). The diffusional mechanisms are predicted to dominate creep deformation for a large range of test temperatures and applied stresses due to the small grain size. μ is the shear modulus.

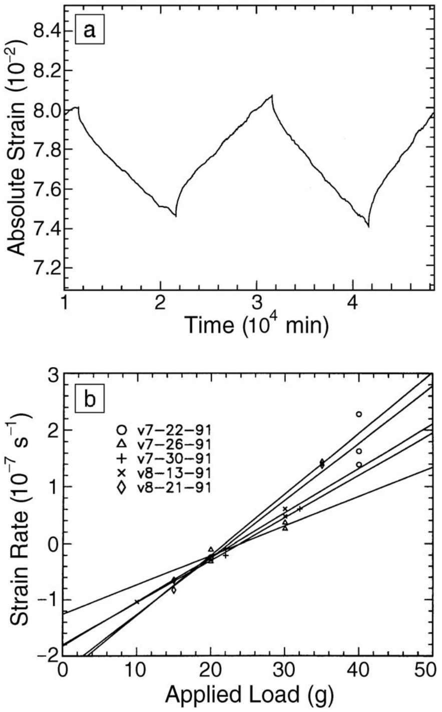

Figure 3. (a) Creep deformation for a Ag/Ni multilayer composed of 15 bilayers; total film thickness is 20 μm and width is 1 cm (from Reference 25). The applied load was changed between 0.1 N and 0.3 N (corresponding to 10 g and 30 g) every ~10^4 min. Negative strain rates were recorded at 0.1 N. (b) Strain rate versus applied load for five Ag/Ni multilayer specimens, each with 21 bilayers; total film thickness is 24 μm and width is 1 cm (from Reference 25). The applied load at which the strain rate would be zero is ~0.23 N (23 g) for each of the five specimens.

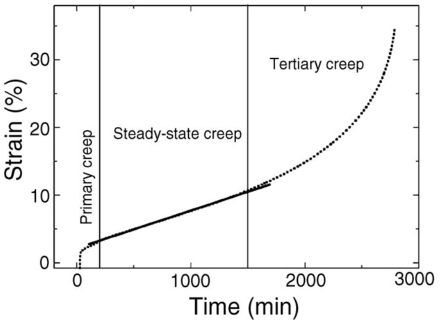

Figure 4. Cumulative strain versus time exhibited by a 150-μm-thick FeCo intermetallic alloy thin film at 600°C with an applied stress of 305 MPa (from Reference 29). Note: even though there are three distinct stages, only the middle, steady-state creep, stage is typically considered.

distinct stages for both bulk and thin-film materials tested in uniaxial tension. During the initial or primary creep stage, strain rates (the local slope of the strain–time curve) usually drop sharply as the material's microstructure (dislocation density, grain shape, etc.) evolves toward a steady state, consistent with the applied load. In the second, or steady-state, stage, microstructure and strain rate remain relatively constant. In the final, or tertiary, stage, the material's microstructure breaks down through the formation of internal voids and cracks, and the global strain rate rises rapidly. Experimental studies of bulk materials typically analyze the steady-state creep stage, and most theories of creep-deformation predict creep rates for this stage. To date, most researchers have applied steady-state creep concepts to the study of thin films. Such application can be misleading.

At 150–260°C and 21 MPa of tension, the primary creep stage for bulk Al encompasses a plastic strain of 18%.[30] In contrast, the maximum total strain, plastic and elastic, that can be induced in an Al film on a Si substrate by heating from 25°C to 500°C is approximately 1%. Thus, almost all of the creep deformation in the Al film might more appropriately be described by primary creep behavior rather than steady-state creep behavior, particularly at lower temperatures.

In contrast, tensile studies of freestanding films allow observation of all stages of creep, although relatively few studies have included analysis of the primary creep stage data (see, e.g., Reference 31). Tensile studies of freestanding Ag/Ni multilayers show that a primary creep stage of 0.1–0.2% precedes the secondary creep stage when the applied stress is changed by ±1 MPa in the temperature range of 650–800°C (as in Figure 3a).[25] The primary creep stage is evident in the steeper slope at the beginning of the curve after each change in applied stress. The magnitude of this strain transient, which is the same for both negative strain rates and positive strain rates, is 1000× larger than the instantaneous elastic strains associated with the stress changes. One might expect this to be particularly significant for film-on-substrate curvature experiments, in which stresses typically vary by hundreds of MPa throughout the experiments, while strains are limited to 1–2%.

Wafer Curvature: Films on Substrates

When thin films on substrates are heated, stresses can rise rapidly. Stress and strain evolution during thermal cycles is modeled by assuming that plastic deformation occurs in the film by the dominant creep mechanism while the substrate remains elastic. Stress–temperature plots generally predict dislocation-creep mechanisms to dominate at the higher stresses and diffusional-creep mechanisms to dominate at the lower stresses (Figure 5). For 1-μm-thick Cu films on Si substrates, stresses are predicted to rapidly relax by diffusional creep as the temperature increases (Figure 5). Measured stresses do not exhibit this behavior.[32,33]

Recent investigations of diffusional creep in Cu films produced by sputtering and annealing under ultrahigh-vacuum conditions found that the stress–temperature curve of the pure Cu films differs significantly from that of Cu-1at.%Al alloy films, where Al surface segregation and oxidation leads to self-passivation.[34,35] Assuming that the diffusional creep is suppressed by surface passivation in the Cu-1at.%Al alloy films, the difference between these alloy films and the pure Cu films could be quantitatively explained by a constrained diffusional-creep model,[36] in which atoms are incorporated into grain boundaries via surface and grain-boundary diffusion with no sliding and no diffusion at the film/substrate interface. Under these assumptions, grain-boundary diffusion relaxes the stresses near grain boundaries, but leaves a significant level of average stress in the film.

Creep Rates of Multilayers

As with thin films, stress and strain evolution in multilayer materials during thermal cycling has been modeled by assuming that creep deformation occurs simultaneously in each layer by the dominant creep mechanisms.[37–39] The creep behavior is generally complicated, as well as history-dependent, with different deformation mechanisms dominating in the different layers at different temperatures.

In constant-temperature tension experiments, on the other hand, the creep behavior is expected to be more straightforward. Upon loading or heating, the less creep-resistant layer strains plastically and in the process sheds most of the stress that acts upon it to the more creep-resistant layer. Changing elastic strains arising from the changing stresses accommodate the different plastic-strain rates in the layers. This load redistribution continues until, in the steady state, both layers are creeping at the same rate, the slower creeping material now bearing the majority of the applied load. The transient associated with this stress redistribution was noted for Ag/Ni multilayers in the previous section on "Steady-State versus Transient Creep." Predictions concerning steady-state creep

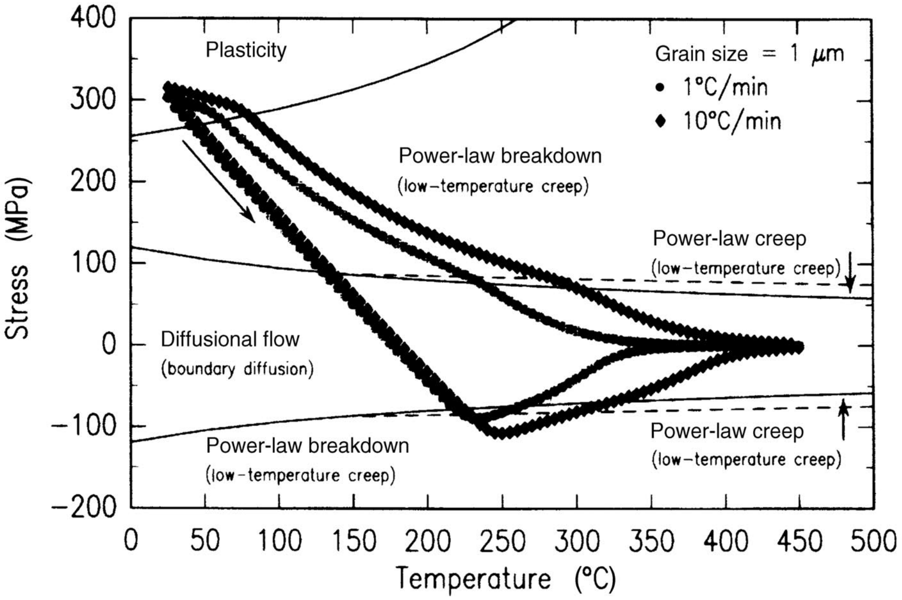

Figure 5. Predicted stress–temperature curves for 1-μm-thick copper films on Si substrates with dominant creep mechanisms indicated (from Reference 32). Heating rate affects the deformation mechanism through its impact on stress relaxation. Note the near-complete stress relaxation at the elevated temperatures.

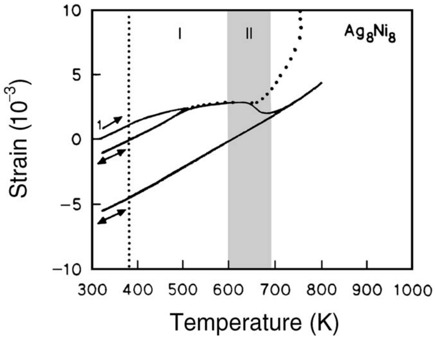

Figure 6. Creep deformation for a Ag_8/Ni_8 multilayer, with layers 2 nm thick (from Reference 41). The applied force was held constant while the temperature was cycled. An applied force of 0.01 N (stress ~0.7 MPa) yielded the solid curve in which the film contracts with each thermal cycle. An applied force of 0.3 N yielded the dotted curve that manifests rapid creep associated with breakdown of the layered structure at the higher temperatures. Structures maintain their layering in region I, but lose it in region II.

rates are now compared to experimental creep results, also for Ag/Ni multilayers.

Using the properties of the slower creeping Ni in the expression for Coble creep,[23]

$$\dot{\varepsilon} = \frac{42\Omega \pi D_b \delta}{kT d^3}(\sigma - \sigma_0), \tag{3}$$

where the zero-creep stress σ_0 has been added,[25] one can predict the strain rate $\dot{\varepsilon}$. Predictions are compared with the experimental data from two groups in Table II. The first group studied Ag/Ni multilayers with layers of the order of 1 μm in thickness.[25] Note the negative strain rates for the lower tensile stress. The values in Table II are for the creep data in Figure 3a. The second group studied Ag/Ni multilayers with layers of the order of 1 nm in thickness.[40,41] Thermal-cycling creep results for multilayers that had only eight atomic planes per elemental layer are shown in Figure 6. Note the shrinkage during thermal cycling for the tensile load.[41] Table II includes an approximate strain rate from constant-temperature creep studies with this specimen.[41] The zero-creep stresses used in Table II come from the creep data in Figure 3a for the ~1-μm-thick layers and from γ/t for the ~1-nm thick layers.

The experimental data for the two Ag/Ni multilayers are inconsistent in both sign and magnitude with the values that are predicted when zero-creep stresses are ignored (Table II). Including the zero-creep stresses makes all experimental and predicted creep rates agree in sign. However, predicted strain rates are still far higher than those measured experimentally, regardless of the omission (inclusion) of the zero-creep stress: 5 (5) orders of magnitude for the ~1-μm-thick layers and 7 (10) orders of magnitude for the ~1-nm-thick layers.

Note that the *sign* of the creep rate is determined by *energetics,* that is, whether contraction or expansion lowers the free energy of the system. The *magnitude* of the creep rate is a manifestation of the *kinetics,* that is, how quickly matter moves in response to the forces driving creep. The fact that experimental and predicted creep rates agree in sign only when zero-creep stresses are accounted for confirms the impact of these stresses on the creep of thin films and layers. The substantial disagreement in the magnitudes of experimental and predicted creep rates, which worsens as grains decrease in size, demonstrates the potential for user error if creep-deformation maps are taken as gospel. Creep studies that correlate stress, strain rate, and temperature for thin-film samples with small but stable grain sizes are evidently needed.

Table II: Comparison of Experimental and Calculated Strain Rates for Ag/Ni Multilayers.

Experimental Data	$\dot{\varepsilon}_{exp.}$ (s^{-1})	σ (MPa)	$\dot{\varepsilon}_{calc.}$ (s^{-1}) for $\sigma_0 = 0$	$\sigma - \sigma_0$ (MPa)	$\dot{\varepsilon}_{calc.}$ (s^{-1}) including σ_0	d (nm)	T (K)
Layer thickness of the order of 1 μm (Reference 25)	-8×10^{-9} $+8 \times 10^{-9}$	0.5 1.5	2×10^{-4} 6×10^{-4}	−0.5 0.5	-2×10^{-4} $+2 \times 10^{-4}$	670	925
Layer thickness of the order of 1 nm (Reference 40)	-1×10^{-8} s^{-1}	0.7	2.0×10^{-1}	−500	-1.5×10^{2}	2	525

Notes: Comparison of experimental strain rates with predictions obtained using deformation mechanism map parameters for Ni with grain size d.[23] Inclusion of zero-creep stress leads to agreement in sign of predicted and experimental strain rates. It does not rectify the difference in rates. $\dot{\varepsilon}_{exp.}$ is the experimentally derived strain rate, σ is the applied stress, $\dot{\varepsilon}_{calc.}$ is the calculated strain rate, σ_o is the zero-creep stress, and T is temperature.

Conclusion

We have outlined the role that diffusional processes play in the creep deformation of thin films. In doing so, we have tried to highlight some of the difficulties encountered in applying concepts originally derived for bulk materials to thin films and multilayers. We have seen that the inclusion of a zero-creep stress is necessary for analyzing and predicting the sign of creep rates. These same results have made clear the shortcomings of extending deformation-mechanism maps, which are based on bulk properties, to multilayer geometries for the prediction of actual creep rates. We have also discussed the existence and magnitude of transients associated with the primary creep regime as well as the implications for thermal-cycling studies of elemental thin films adhering to substrates. In summary, extreme caution should be used in applying the general concepts of steady-state creep behavior of bulk materials to the analysis of thin-film deformation at elevated temperatures.

Acknowledgment

This work is funded in part by DOE/OBES grant No. DE-FG-0297-ER45664 and AFOSR award No. F49620-00-1-0028.

References

1. J. Schiøtz, T. Vegge, F.D. Di Tolla, and K.W. Jacobsen, *Phys. Rev. B* **60** (1999) p. 11971.
2. W.N. Sharpe, B. Yuan, and R.L. Edwards, *J. Microelectromech. Sys.* **6** (1997) p. 193.
3. O. Kraft and C.A. Volkert, *Adv. Eng. Mater.* **3** (2001) p. 99.
4. T.P. Weihs, S. Hong, J.C. Bravman, and W.D. Nix, *J. Mater. Res.* **3** (1988) p. 931.
5. W.D. Nix, *Metall. Trans. A* **20A** (1989) p. 2217.
6. M. Hommel, O. Kraft, and E. Arzt, *J. Mater. Res.* **14** (1999) p. 2373.
7. A.G. Atkins, A. Silverio, and D. Tabor, *J. Inst. Met.* **94** (1966) p. 369.
8. S.N.G. Chu and J.C.M. Li, *J. Mater. Sci.* **12** (1977) p. 2200.
9. D. Stone, W.R. Lafontaine, P. Alexopoulos, and C.Y. Li, *J. Mater. Res.* **3** (1988) p. 141.
10. V. Raman and R. Berriche, *J. Mater. Res.* **7** (1992) p. 627.
11. M.D. Thouless, *Acta Metall. Mater.* **41** (1993) p. 1057.
12. K.T. Miller, F.F. Lange, and D.B. Marshall, *J. Mater. Res.* **5** (1990) p. 151.
13. F.Y. Genin, W.W. Mullins, and P. Wynblatt, *Acta Metall. Mater.* **40** (1992) p. 3239.
14. D.J. Srolovitz and S.A. Safran, *J. Appl. Phys.* **60** (1986) p. 247.
15. D.J. Srolovitz and S.A. Safran, *J. Appl. Phys.* **60** (1986) p. 255.
16. D. Josell and W.C. Carter, in *Creep and Stress Relaxation in Miniature Structures and Components,* edited by H.D. Merchant (The Minerals, Metals, and Materials Society, Warrendale, PA, 1996) p. 271.
17. D. Josell, S.R. Coriell, and G.B. McFadden, *Acta Metall. Mater.* **43** (1995) p. 1987.
18. J.P. Fain, R. Banerjee, D. Josell, P.M. Anderson, H. Fraser, N. Tymiak, and W. Gerberich, in *Nanophase and Nanocomposite Materials III,* edited by S. Komarneni, J.C. Parker, and H. Hahn (Mater. Res. Soc. Symp. Proc. **581**, Warrendale, PA, 2000) p. 603.
19. D. Josell, W.C. Carter, and J.E. Bonevich, *Nanostruct. Mater.* **12** (1999) p. 387.
20. A.C. Lewis, A.B. Mann, D. Josell, J. Tapson, and T.P. Weihs, in *Interfacial Engineering for Optimized Properties II,* edited by C.B. Carter, E.L. Hall, S.R. Nutt, and C.L. Briant (Mater. Res. Soc. Symp. Proc. **586**, Warrendale, PA, 2000) p. 249.
21. T.H. Courtney, *Mechanical Behavior of Materials* (McGraw-Hill, New York, 2000).
22. G.B. Gibbs, *Philos. Mag.* **13** (1966) p. 589.
23. H.J. Frost and M.F. Ashby, *Deformation-Mechanism Maps: The Plasticity and Creep of Metals and Ceramics* (Pergamon Press, New York, 1982).
24. D. Josell and F. Spaepen, *Acta Metall. Mater.* **41** (1993) p. 3007.
25. D. Josell and F. Spaepen, *Acta Metall. Mater.* **41** (1993) p. 3017.
26. D. Josell and Z.L. Wang, in *Thin Films: Stresses and Mechanical Properties V,* edited by S.P. Baker, C.A. Ross, P.H. Townsend, C.A. Volkert, and P. Børgesen (Mater. Res. Soc. Symp. Proc. **356**, Pittsburgh, 1995) p. 357.
27. K.E. Harris and A.H. King, *Acta Mater.* **46** (1998) p. 6195.
28. A.C. Lewis, A.B. Mann, D. van Heerden, D. Josell, and T.P. Weihs, in *Influences of Interface and Dislocation Behavior on Microstructure Evolution,* edited by M. Aindow, M.D. Asta, M.V. Glazov, D.L. Medlin, A.D. Rollet, and M. Zaiser (Mater. Res. Soc. Symp. Proc. **652**, Warrendale, PA, 2001) p. Y1.3.1.
29. C.H. Shang, R.C. Cammarata, C.L. Chien, and T.P. Weihs, *Acta. Mater.* (2001) to be submitted.
30. O.D. Sherby and P.M. Burke, *Prog. Mater. Sci.* **13** (1968) p. 325.
31. F.R. Brotzen, C.T. Rosenmayer, C.G. Cofer, and R.J. Gale, *Vacuum* **41** (1990) p. 1287.
32. M.D. Thouless, J. Gupta, and J.M.E. Harper, *J. Mater. Res.* **8** (1993) p. 1845.
33. R.-M. Keller, S.P. Baker, and E. Arzt, *Acta Mater.* **47** (1999) p. 415.
34. E. Arzt, G. Dehm, P. Gumbsch, O. Kraft, and D. Weiss, *Prog. Mater. Sci.* **46** (2001) p. 283.
35. D. Weiss, H. Gao, and E. Arzt, *Acta Mater.* **49** (2001) p. 2395.
36. H. Gao, L. Zhang, W.D. Nix, C.V. Thompson, and E. Arzt, *Acta Mater.* **47** (1999) p. 2865.
37. Y.-L. Shen and S. Suresh, *Acta Metall. Mater.* **43** (1995) p. 3915.
38. Y.-L. Shen and S. Suresh, *J. Mater. Res.* **10** (1995) p. 1200.
39. Y.-L. Shen and S. Suresh, *Acta Mater.* **44** (1996) p. 1337.
40. V. Pelosin and J. Hillairet, *Nanostruct. Mater.* **4** (1994) p. 229.
41. V. Pelosin, J. Hillairet, and B. Rodmacq, *J. Phys.: Condens. Matter* **6** (1994) p. 1099. Strain rate obtained from creep data in Figure 8. □